Cell. Mol. Life Sci. 64 (2007) 219–229
1420-682X/07/020219-11
DOI 10.1007/s00018-006-6445-4

Cellular and Molecular Life Sciences

Research Article

Endocannabinoids in adipocytes during differentiation and their role in glucose uptake

V. Gasperi [a, †], F. Fezza [b, c, †], N. Pasquariello [a], M. Bari [b], S. Oddi [a, c], A. Finazzi Agrò [b] and M. Maccarrone [a, c, *]

[a] Department of Biomedical Sciences, University of Teramo, Piazza A. Moro 45, 64100 Teramo (Italy), Fax: +39 0861 412583, e-mail: mmaccarrone@unite.it

[b] Department of Experimental Medicine and Biochemical Sciences, University of Rome 'Tor Vergata', Via Montpellier 1, 00133 Rome (Italy)

[c] European Center for Brain Research (CERC)/IRCCS S. Lucia Foundation, Via del Fosso di Fiorano 64/65, 00143 Rome (Italy)

Received 11 October 2006; received after revision 9 November 2006; accepted 28 November 2006
Online First 22 December 2006

Abstract. The molecular basis for the control of energy balance by the endocannabinoid anandamide (AEA) is still unclear. Here, we show that murine 3T3-L1 fibroblasts have the machinery to bind, synthesize and degrade AEA, and that their differentiation into adipocytes increases by approximately twofold the binding efficiency of cannabinoid receptors (CBR), and by approximately twofold and approximately threefold, respectively, the catalytic efficiency of the AEA transporter and AEA hydrolase. In contrast, the activity of the AEA synthetase and the binding efficiency of vanilloid receptor were not affected by the differentiation process. In addition, we demonstrate that AEA increases by approximately twofold insulin-stimulated glucose uptake in differentiated adipocytes, according to a CB1R-dependent mechanism that involves nitric oxide synthase, but not lipoxygenase or cyclooxygenase. We also show that AEA binding to peroxisome proliferator-activated receptor-γ, known to induce differentiation of 3T3-L1 fibroblasts into adipocytes, is not involved in the stimulation of glucose uptake.

Keywords. Differentiation, endocannabinoid system, energy homeostasis, glucose transport, receptor, signal transduction.

Introduction

Cannabinoids are the bioactive constituents of *Cannabis sativa* extracts like hashish and marijuana. The effects of these substances on the central nervous system and peripheral tissues have been known for centuries, and are due to the activation of cannabinoid (CB) receptors [1, 2]. The endogenous agonists of these receptors are amides and esters of long-chain polyunsaturated fatty acids, collectively termed 'endocannabinoids' [3]. Anandamide (*N*-arachidonoylethanolamine, AEA) and 2-arachidonoylglycerol (2-AG) are the most prominent endocannabinoids as yet known [3]. AEA is synthesized on demand by *N*-acyl-phosphatidylethanolamines-hydrolyzing phospholipase D (NAPE-PLD) [4], and is effective primarily at type-1 (CB1R) and type-2 (CB2R) cannabinoid receptors [1, 2]. In addition, the type-1 vanilloid receptors (now called transient receptor potential channel vanilloid receptor subunit 1, TRPV1) are activated by AEA, which therefore is considered also a true 'endovanilloid' [5]. The biological activities of AEA are terminated by cellular uptake through a purported AEA membrane transporter (AMT) [6–8], followed by intracellular degrada-

* Corresponding author.
† These authors equally contributed to the study.

tion by fatty acid amide hydrolase (FAAH) [9]. AEA and congeners, together with (non)CB receptors, NAPE-PLD, AMT and FAAH form the 'endocannabinoid system', which plays roles in a broad array of physiological and pathological processes [1, 3, 5].

In the past few years, evidence has been accumulated for a role of the endocannabinoid system in controlling energy balance, through central and peripheral actions [10–13]. An increase of the endocannabinoid tone has been reported in the hypothalamus of obese animals, and the administration of (endo)cannabinoids has been shown to increase food intake and to promote weight gain [14–17]. In white adipocytes, CB1R activation stimulates lipogenesis, by up-regulating lipoprotein-lipase [11, 14] and fatty acid synthesis, which contributes to diet-induced obesity *in vivo* [18]. In contrast, CB1R antagonists *in vitro* and *in vivo* cause the up-regulation of adiponectin, which in turn reduces the expression of enzymes involved in lipogenesis [19, 20]. In line with the latter observation, the CB1R antagonist SR141716A (rimonabant) has been shown to effectively reduce food intake and to decrease body weight in late-stage clinical trials, thus approaching the market as an anti-obesity drug [21, 22]. The therapeutic efficacy of rimonabant in humans has found biochemical support in the observation that human adipose tissue has CB1 receptors [23–25] and a functional endocannabinoid system [25]. In this context, AEA has been recently shown to induce fibroblast differentiation into adipocytes, through transcriptional activation of peroxisome proliferator-activated receptor-γ (PPARγ) [26]. However, up to now, only one report has appeared, during the preparation of this manuscript, describing that murine 3T3-L1 preadipocytes express the genes encoding for CB1R, CB2R, NAPE-PLD, and FAAH [27]. Therefore, the modulation of the endocannabinoid system during adipocyte differentiation, and the role of endocannabinoids on glucose uptake by adipocytes remain to be clarified. Both adipocyte differentiation and glucose transport are key processes in adipogenesis and maintenance of energy balance and body weight [26, 28].

This background prompted us to investigate the presence of a complete and functional AEA-related endocannabinoid system in murine 3T3-L1 preadipocytes, and to investigate the effect of cell differentiation on this system. In addition, we sought to ascertain the potential role of AEA in glucose uptake by 3T3-L1 adipocytes, and the underlying mechanism. In this context, it should be recalled that arachidonic acid (AA) significantly increases basal and insulin-stimulated glucose uptake in murine adipocytes [28], and that AA derivatives generated by cyclooxygenase-2 (COX-2) or lipoxygenase (LOX) interfere with adipocyte metabolism [29–32]. Therefore, we checked whether the FAAH-catalyzed release of AA from AEA [9], and the oxygenation of AEA by COX-2 [33] or LOX [34], might have a role in modulating glucose uptake. The potential involvement of PPARγ in AEA-stimulated glucose uptake was also investigated, because activation of this receptor is known to control glucose homeostasis in adipocytes [35].

Materials and methods

Materials. Chemicals were of the purest analytical grade. AEA, AA, capsazepine (CPZ), 2-deoxy-D-glucose (2-DOG), dexametasone, GW9662, indomethacin (INDO), insulin, isobutylmethylxanthine, *N*-ω-nitro-L-arginine methyl ester (L-NAME), nordihydroguaiaretic acid (NDGA), rosiglitazone (RSG), 5-(1,1′-dimethyheptyl)-2-[1*R*,5*R*-hydroxy-2*R*-(3-hydroxypropyl)cyclohexyl]-phenol (CP55.940), and sodium nitroprusside (SNP) were purchased from Sigma Chemical Co. (St. Louis, MO, USA). Resinferatoxin (RTX) was from Alexis Corporation (Lausen, Switzerland), and methanandamide (Met-AEA) was from Calbiochem (La Jolla, CA, USA). (*S*)-1′-(4-Hydroxybenzyl)-oleoylethanolamide (OMDM1), arachidonoyl-2-chloro-ethylamide (ACEA) and methyl arachidonyl fluorophosphonate (MAFP) were from Tocris (Bristol, United Kingdom). *N*-Piperidino-5-(4-chlorophenyl)-1-(2,4-dichlorophenyl)-4-methyl-3-pyrazolecarboxamide (SR141716A) and *N*-[1(*S*)-endo-1,3,3-trimethylbicyclo[2.2.1]-heptan-2-yl]-5-(4-chloro-3-methylphenyl)-1-(4-methylbenzyl) pyrazole-3-carboxami-de (SR144528) were kind gifts of Sanofi-Aventis Recherche (Montpellier, France). Pure FAAH was a kind gift of Dr Benjamin F. Cravatt (The Scripps Research Institute, La Jolla, CA, USA). *N*-Arachidonoyl-phosphatidyl-ethanolamine (NArPE) was synthesized from AA and phosphatidylethanolamine, as reported [35]. [^{3}H]AEA (205 Ci/mmol), 2-deoxy-D-[2,6-^{3}H]glucose ([^{3}H]2-DOG, 29.7 Ci/mmol), [^{3}H]CP55.940 (126 Ci/mmol), and [^{3}H]resinferatoxin ([^{3}H]RTX, 43 Ci/mmol) were from Perkin-Elmer Life Sciences, Inc. (Boston, MA, USA). [^{3}H]NArPE (200 Ci/mmol) was from ARC (St. Louis, MO, USA). Anti-FAAH polyclonal antibodies were prepared by Primm S.r.l. (Milan, Italy) as reported [36]. Rabbit anti-CB1R and mouse anti-inducible nitric oxide synthase (iNOS) antibodies were from Affinity BioReagents (Golden, CO, USA). Rabbit anti-CB2R antibodies were from Cayman Chemicals (Ann Arbor, MI, USA), and rabbit anti-TRPV1 antibodies were from Santa Cruz Biotechnologies (Santa Cruz, CA, USA). Goat anti-rabbit and goat anti-mouse antibodies conjugated to alkaline phosphatase (GAR-AP and GAM-AP, respectively) were from Bio-Rad (Hercules, CA, USA).

Cell culture and treatment. Mouse 3T3-L1 fibroblasts were purchased from American Type Culture Collection (ATCC, Manassas, VA, USA) and were either maintained as such or differentiated into adipocytes, as reported [20]. Fibroblasts were maintained at ≤70% confluency in Dulbecco's minimal essential medium (DMEM, Sigma), containing 10% newborn calf serum (NCS), 25 mM glucose, 2 mM glutamine, 18 mM disodium bicarbonate, 100 U/ml penicillin, and 100 μg/ml streptomycin, at 37 °C in humidified 5% CO_2 atmosphere. To differentiate fibroblasts into mature adipocytes, 3T3-L1 cells were grown for 2 days post confluence in DMEM/NCS, and then for 2 additional days in medium containing fetal bovine serum instead of NCS (DMEM/FBS), 0.83 μM insulin, 0.25 μM dexamethasone and 0.5 mM isobutylmethylxanthine. The medium was changed to DMEM/FBS supplemented only with 0.83 μM insulin for 2 days, and then to DMEM/FBS alone for additional 3–5 days. Cells were considered differentiated, when at least 95% of them showed an adipocyte phenotype by accumulation of lipid droplets, usually on day 9 (d9) of differentiation [28].

Receptor binding assays. For cannabinoid receptor studies, membrane fractions were prepared from 3T3-L1 cells as reported [36], and were stored at –80 °C for no longer than 1 week. Membrane fractions were used in rapid filtration assays with the synthetic cannabinoid [^{3}H]CP55.940 [36]. To assess the presence of TRPV1, binding of [^{3}H]RTX to membrane fractions was determined by rapid filtration assays, as described previously [37]. In all binding experiments, nonspecific binding was determined in the presence of 1 μM 'cold' agonist [36, 37]. Receptor binding was expressed as fmol ^{3}H-labeled ligand bound per mg protein. Binding data were elaborated through nonlinear regression analysis, using the Prism 4 program (GraphPAD Software for Science, San Diego, CA, USA), to calculate apparent dissociation constant (K_d) and maximum binding (B_{max}) of [^{3}H]CP55.940 or [^{3}H]RTX.

The expression of CB1R, CB2R and TRPV1 was assessed in 3T3-L1 cell extracts, subjected to 10% SDS-PAGE (10 μg/lane) under reducing conditions. For immunochemical analysis, gels were electroblotted onto 0.45- μm nitrocellulose filters (Bio-Rad) and were immunoreacted with anti-CB1R, anti-CB2R (each diluted 1 : 250) or anti-TRPV1 (1 : 500) polyclonal antibodies, and GAR-AP (diluted 1 : 2000) as second antibody [38]. In addition, Western blot analysis of CB1R and CB2R was performed under the same experimental conditions on mouse brain and mouse spleen extracts, typical sources of authentic CB1R and CB2R, respectively [39]. Anti-CB1R and CB2R antibodies (each diluted 1 : 250), anti-TRPV1 antibody (1 : 500), and GAR-AP (diluted 1 : 2000) were used to determine CB1R, CB2R and TRPV1 protein content also by enzyme-linked immunosorbent assay (ELISA), coating wells with cell extracts (20 μg/well), as reported [38]. The absorbance values at 405 nm (A_{405}) of unknown samples were within the linearity range of calibration curves drawn with different amounts of extracts (in the range 0–40 μg/well).

For the evaluation of PPARγ binding, the PolarScreen™ PPAR Competitor Assay kit was used (Invitrogen Co. Carlsbad, CA, USA) [26]. This assay is based on human-derived recombinant PPARγ ligand-binding domain (PPARγ-LBD), tagged with an N-terminal His-tag, and a tight-binding selective fluorescent PPAR ligand (Fluormone PPAR Green). PPARγ-LBD was added to Fluormone™ PPAR Green, to form a PPARγ-LBD/Fluormone™ PPAR Green complex, which results in high fluorescence polarization. The effect of AEA or rosiglitazone (RSG), in the range 0.001–100 μM, on complex formation was ascertained in microwell plates at room temperature for 2 h, and fluorescence polarization was measured using LS-50B Luminescence Spectrometer (Perkin-Elmer, Boston, MA, USA), with excitation at 517 nm and emission at 535 nm.

FAAH activity and expression. The hydrolysis of [^{3}H]AEA by FAAH (EC 3.5.1.4) was assayed in 3T3-L1 cell homogenates (10 μg/test), incubated at pH 9.0 with 10 μM [^{3}H]AEA. The release of [^{3}H]AA from [^{3}H]AEA was evaluated through reversed phase-high performance liquid chromatography (RP-HPLC), as already reported [38]. The apparent Michaelis-Menten constant (K_m) and maximum velocity (V_{max}) of FAAH were calculated by nonlinear regression analysis with the Prism 4 program (GraphPAD Software for Science).

FAAH expression was determined in 3T3-L1 cell extracts by Western blot analysis, as described above for CBR and TRPV1 receptors. Anti-FAAH polyclonal antibodies (1 : 250) and GAR-AP (diluted 1 : 2000) were used to visualize the immunoreactive bands, and pure FAAH (3 μg/lane) was used as positive control. The same anti-FAAH antibodies (diluted 1 : 200) were used to determine FAAH protein content by ELISA, performed as described above for CB receptors.

Anandamide synthesis and uptake. The synthesis of AEA through the activity of NAPE-PLD (EC 3.1.4.4) was assayed in cell homogenates (100 μg/test), using 100 μM [^{3}H]NArPE as detailed elsewhere [40]. NAPE-PLD activity was expressed as pmol [^{3}H]AEA released per min per mg protein. The uptake of [^{3}H]AEA through AMT was measured by incubating intact 3T3-L1 cells (1.5×10^6 cells/test) with 1 μM [^{3}H]AEA, at 37 °C for 15 min [38]. To discriminate noncarrier-mediated from carrier-mediated transport of AEA, control experiments were carried out also at 4 °C, and these values were subtracted from those at 37 °C [6]. Incubations were also carried out with different concentrations of [^{3}H]AEA, in the range 0–2 μM, to determine apparent K_m and V_{max} values, by nonlinear regression analysis (Prism 4).

Assay of 2-DOG uptake. 3T3-L1 adipocytes (on d8 of differentiation) were grown in six-well plates and were incubated for 24 h in supplemented DMEM. In the time course experiments, AEA incubations started on d7 and d9 and continued for 48 or 4 h, respectively. All the treatments were performed at the concentrations indicated in the figure legends.

[^{3}H]2-DOG uptake was performed on d9, as reported previously [41]. Differentiated adipocytes were serum-starved for 2 h in DMEM containing 25 mM glucose and 2 mM glutamine, and were incubated in 1 ml KRH buffer (136 mM NaCl, 4.7 mM KCl, 1.25 mM $CaCl_2$, 1.25 mM $MgSO_4$, 10 mM HEPES, pH 7.4), with or without 100 nM insulin, at 37 °C for 30 min. Then, [^{3}H]2-DOG (0.3 µCi/ml; final specific activity 6 µCi/ µmol) was added for an additional 5 min. Uptake was stopped by three rapid washes on ice with KRH, then cells were solubilized in 1 ml 0.1 M NaOH, were neutralized with 50 µl concentrated HCl, and radioactivity was determined by liquid scintillation counting.

Expression of iNOS. The expression of iNOS in 3T3-L1 cells was assessed by Western blot analysis, performed as described above for CBR and TRPV1 receptors. Mouse anti-iNOS monoclonal antibody was used as first antibody (diluted 1 : 5000), and GAM-AP (diluted 1 : 2000) as second antibody [38]. Lysates from mouse macrophages stimulated with interferon-γ (IFN-γ) and lipopolysaccharide (LPS) for 12 h were used as positive control [42].

Statistical analysis. Data reported in this article are the means ± SD of at least three independent experiments, each performed in duplicate. Statistical analysis was performed by the nonparametric Mann-Whitney U test, elaborating experimental data by means of the InStat 3 program (GraphPAD Software for Science).

Results

AEA-binding receptors in 3T3-L1 cells during differentiation. In a first series of experiments, aimed at looking for a complete endocannabinoid system in 3T3-L1 cells, the presence of AEA-binding receptors was investigated. Binding assays were performed with the synthetic agonist [^{3}H]CP55.940, which has high affinity to both CB1 and CB2 receptors [39]. [^{3}H]CP55.940 was able to bind dose-dependently to 3T3-L1 cell membranes, both before (d0) and after 9 days (d9) of differentiation (Fig. 1a). From saturation curves like those shown in Figure 1a, it was possible to calculate the apparent affinity (*i.e.* the dissociation constant, K_d) and maximum binding (B_{max}) of the receptor, and hence its binding efficiency (*i.e.* the B_{max}/K_d ratio) (Table 1). Interestingly the latter parameter, which is an overall index of receptor functionality, was almost doubled in differentiated adipocytes versus preadipocytes (Table 1). Furthermore, [^{3}H]CP55.940 (400 pM) was displaced by 1 µM SR141716A (down to 50% or 30% of controls on d0 or d9, respectively), or by 1 µM SR144528 (down to 50% or 70% of controls on d0 or d9, respectively). These compounds are selective antagonists of CB1R (SR141716A) or CB2R (SR144528) [39]. The effect of these antagonists, and the fact that the apparent K_d values of [^{3}H]CP55.940 binding are compatible with both CB1 and CB2 receptor subtypes [39], suggested that both CB receptors were expressed in 3T3-L1 cells. To further corroborate the binding data, 3T3-L1 cell extracts were subjected to Western blot analysis, which was extended to mouse brain and spleen, typical sources of authentic CB1R and CB2R, respectively [39]. Anti-CB1R and anti-CB2R antibodies were found to recognize a single immunoreactive band of the expected molecular size of CB1 and CB2 receptors, respectively (Fig. 2a, b). In addition, Western blot analysis suggested that CB1R expression increased during differentiation, whereas CB2R had an opposite trend (Fig. 2a, b). More quantitative ELISA were performed, to further corroborate this observation, and demonstrated that CB1R protein was almost doubled in 3T3-L1 cells on d9 versus d0 (1.700 ± 0.130 versus 0.920 ± 0.070 A_{405} units per µg protein; $p < 0.01$), whereas the level of CB2R was reduced down to ~45% (from 0.750 ± 0.050 to 0.340 ± 0.040 A_{405} units per µg protein; $p < 0.01$).

Adipocyte cell membranes were also able to dose-dependently bind [^{3}H]RTX, a specific TRPV1 agonist [36] (Fig. 1b). The binding of 500 pM [^{3}H]RTX was fully displaced by 1 µM CPZ (down to 30% of controls, both on d0 and d9), a selective antagonist of TRPV1 receptor [37]. Kinetic analysis of TRPV1 saturation curves yielded apparent K_d and B_{max} values reported in Table 1, demonstrating that the binding efficiency of TRPV1 did not change during differentiation. The presence of vanilloid receptors in 3T3-L1 cells was further established by Western blot analysis, using human lymphoma U937 cells as a positive control [43]. Western blotting showed a single immunoreactive band of the expected molecular size of TRPV1, and suggested that band intensity did not change during differentiation (Fig. 2c). ELISA, showing that protein content of TRPV1 remained the same in 3T3-L1 cells on d9 versus d0 (~0.330 ± 0.040 A_{405} units per µg protein in each case), confirmed the Western blotting data.

Taken together, these biochemical and immunochemical data demonstrate that both 3T3-L1 preadipocytes and adipocytes express functional CB1R, CB2R and TRPV1. They also show that differentiation affects CBR binding efficiency, by enhancing the expression of CB1R and reducing that of CB2R, while the binding efficiency and expression of TRPV1 were unmodified.

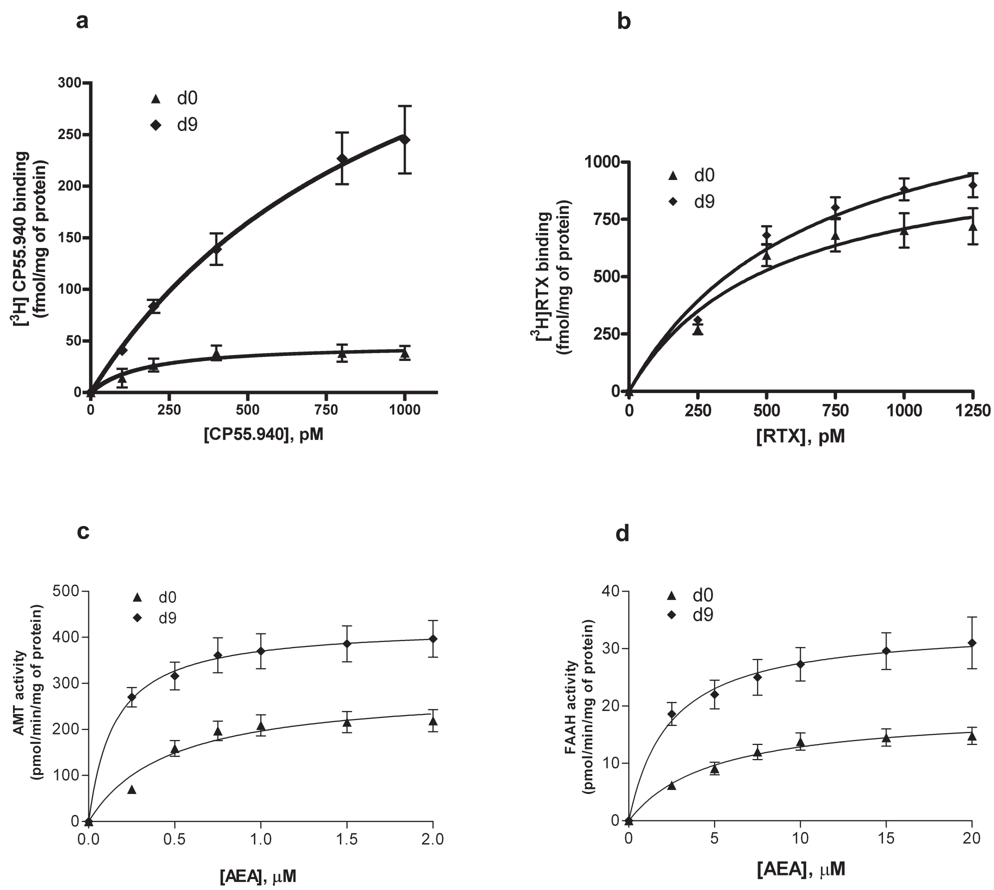

Figure 1. Endocannabinoid system in 3T3-L1 cells during differentiation. Saturation curves of the binding of [^{3}H]CP55.940 (*a*) or [^{3}H]resinferatoxin (RTX) (*b*) at the beginning (d0) and on day 9 of differentiation (d9). Dependence of AMT activity (*c*) and of fatty acid amide hydrolase (FAAH) activity (*d*) on anandamide (AEA) concentration, on d0 and d9. Vertical bars represent SD values.

Table 1. Kinetic properties of the endocannabinoid system in 3T3-L1 cells during differentiation.

Parameter	d0 [a]			d9 [b]		
	K_d [c]	B_{max} [d]	B_{max}/K_d	K_d [c]	B_{max} [d]	B_{max}/K_d
CBR binding	0.20 ± 0.05	47.4 ± 6.1	237	1.1 ± 0.4	510 ± 29	463
TRPV1 binding	520 ± 31	1077 ± 216	2.1	671 ± 32	1451 ± 245	2.2
	K_m [e]	V_{max} [f]	V_{max}/K_m	K_m [e]	V_{max} [f]	V_{max}/K_m
FAAH activity	4.9 ± 0.6	19.2 ± 1.6	3.9	2.4 ± 0.3	33. 8 ± 4.1	14.1
AMT activity	0.11 ± 0.02	23.3 ± 4.0	212	0.03 ± 0.06	16.1 ± 3.1	537

[a] At the beginning of differentiation.
[b] On day 9 of differentiation.
[c] Expressed as nM.
[d] Expressed as fmol per mg protein.
[e] Expressed as μM.
[f] Expressed as pmol/min per mg protein.

AEA metabolism in 3T3-L1 cells during differentiation. 3T3-L1 cells at the preadipocyte and adipocyte stage were able to accumulate [^{3}H]AEA concentration-dependently (Fig. 1c), according to a saturable process typical of AMT [6–8, 44]. From saturation curves like those shown in Figure 1c, it was possible to calculate the apparent affinity (i.e. K_m) and maximum velocity (V_{max}) of AMT, and therefore it could be demonstrated that differentiation almost doubled the catalytic efficiency (i.e. V_{max}/K_m ratio) of the transporter (Table 1). The uptake of 1 μM [^{3}H]AEA was inhibited (down to ~10% of control) by 1 μM OMDM1, a selective AMT inhibitor [45],

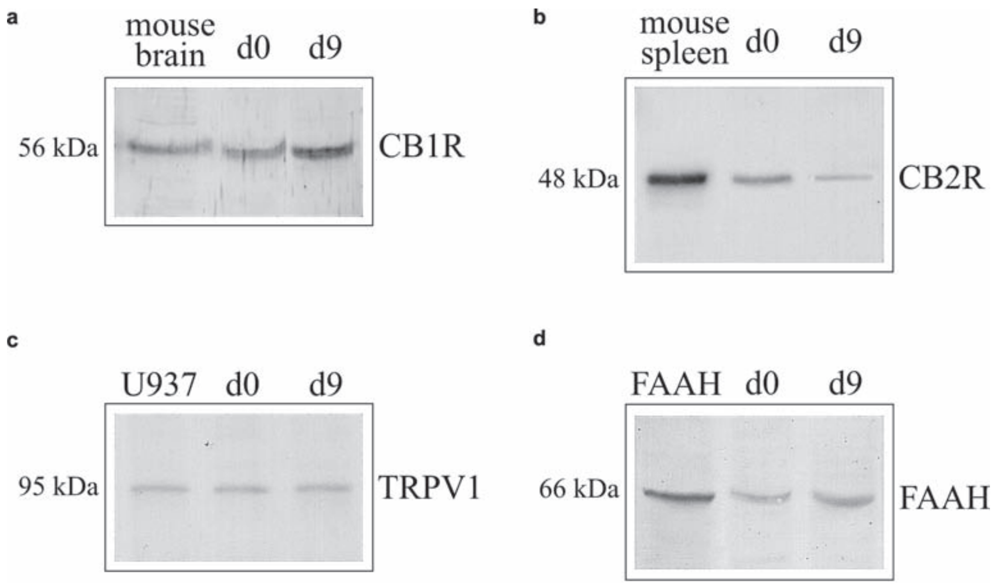

Figure 2. Western blot of cannabinoid and vanilloid receptors, and of FAAH in 3T3-L1 cells. Western blot analysis in 3T3-L1 membranes, reacted with anti-CB1R (*a*), anti-CB2R (*b*), anti-TRPV1 (*c*), or anti-FAAH (*d*) polyclonal antibodies. Expected molecular mass values are reported on the left-hand side.

whereas 2-DOG was ineffective up to a concentration of 50 µM (not shown). Furthermore, 3T3-L1 cells were able to synthesize *de novo* AEA through NAPE-PLD activity (15 ± 3 pmol/min per mg protein, at either d0 and d9 of differentiation). It should be stressed that the unprecedented observation of an active AEA synthetase in 3T3-L1 adipocytes gives support to a recent report that appeared during the preparation of this manuscript, showing that 3T3-L1 cells express detectable levels of endogenous AEA [27].

3T3-L1 cells at d0 or d9 were also able to hydrolyze [^{3}H]AEA through FAAH activity, according to a typical Michaelis-Menten kinetics (Fig. 1d). From curves like those shown in Figure 1d, it was possible to calculate K_m and V_{max} values, and hence the catalytic efficiency (i.e. V_{max}/K_m ratio) of FAAH (Table 1). This kinetic analysis demonstrated that differentiation increased by ~3.5-fold the catalytic efficiency of FAAH on d9 *versus* d0 (Table 1). As expected, hydrolysis of 10 µM [^{3}H]AEA was almost completely inhibited by 100 nM MAFP (down to ~10% of controls), a selective inhibitor of FAAH [46]. The presence of FAAH in 3T3-L1 cells was also demonstrated by Western blot where specific antibodies recognized a single immunoreactive band of the molecular size expected for FAAH (Fig. 2d). In addition, Western blotting suggested that the intensity of the FAAH-immunoreactive band increased during differentiation (Fig. 2d), and ELISA supported this finding, demonstrating that FAAH protein increased up to ~160% (0.770 ± 0.055 *versus* 0.480 ± 0.030 A_{405} units per µg protein; $p < 0.01$) in 3T3-L1 cells on d9 *versus* d0.

Taken together, these biochemical and immunochemical data demonstrate that both 3T3-L1 preadipocytes and adipocytes have the whole machinery to metabolize AEA, and suggest that differentiation increases the degradation of this endocannabinoid via AMT and FAAH, without affecting its synthesis via NAPE-PLD.

Modulation of 2-DOG uptake by AEA in 3T3-L1 adipocytes. Growing evidence suggests that endocannabinoids play a major role in controlling food intake and body weight [10–13, 47]. In this line, we sought to test the effect of AEA on basal and insulin-stimulated glucose uptake in derived 3T3-L1 adipocytes. These cells were incubated for 24 h with different concentrations of AEA, and a maximum effect (~160%) on insulin-stimulated uptake was found when used at 10 µM (Fig. 3a). Then, 3T3-L1 adipocytes were incubated with 10 µM AEA for different periods of time (between 4 and 48 h), to clarify the time course of the AEA effect. Glucose (2-DOG) uptake was found to increase significantly after 24 h of treatment, whereas the basal (unstimulated) transport of glucose was not affected, independently of the concentration of AEA (Fig. 3a) and of the duration of the treatment (Fig. 3b). In this context, AA has been shown to increase significantly both basal and insulin-stimulated glucose uptake [28]. Since 3T3-L1 adipocytes are able to efficiently degrade AEA through AMT and FAAH (Fig. 1c, d), thus potentially generating AA, we checked whether the stimulatory effect of AEA on insulin-stimulated glucose uptake could be indeed due to AA. Thus, cells were treated with AEA in the presence of the FAAH inhibitor MAFP (100 nM). Moreover, the effect of Met-AEA, a hydrolytically stable

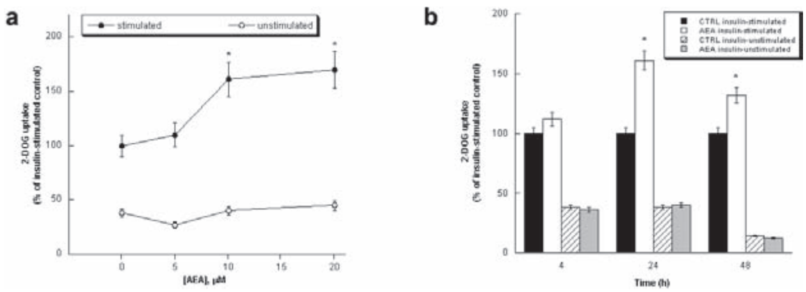

Figure 3. Effect of AEA concentration (*a*), and incubation time (*b*) on basal and insulin-stimulated glucose uptake in differentiated 3T3-L1 cells. (*a*) Values were expressed as percentage of glucose uptake at 24 h in insulin-stimulated control (100% = 302 ± 36 pmol/min per mg protein). (*b*) Values were expressed as percentage of glucose uptake in insulin-stimulated control at the corresponding incubation times, in the presence or absence of 10 μM AEA (100% at 4 h, 556 ± 71 pmol/min per mg protein; 100% at 24 h, 302 ± 36 pmol/min per mg protein; 100% at 48 h, 230 ± 19 pmol/min per mg protein). Vertical bars represent SD values. * $p < 0.01$ *versus* corresponding controls ($p > 0.05$ in all other cases).

analogue of AEA [48], on insulin-stimulated glucose uptake was also checked. We found that the stimulatory effect of 10 μM AEA was not impaired by MAFP, and was mimicked by 1 μM Met-AEA (data not shown), ruling out that AA could be responsible for the activity of AEA. Therefore, we performed further experiments on the effect of SR141716A or SR144528 on AEA-stimulated glucose uptake, by incubating 3T3-L1 cells with 10 μM AEA for 24 h in the presence of 100 nM MAFP. Interestingly, 1 μM SR141716A was shown to reduce the effect of AEA on glucose uptake down to ~50% of that of the controls, whereas 1 μM SR144528 or 10 μM CPZ were ineffective (Fig. 4a). Additionally, glucose uptake was enhanced by 10 μM ACEA (Fig. 4b), a highly selective CB1R agonist [49], and by 10 μM OMDM1 (Fig. 4b), a selective AMT blocker [45].

Taken together, these data suggest that AEA enhances insulin-stimulated glucose uptake through a CB1R-dependent mechanism. Accordingly, inhibition of AEA transport further potentiates the stimulatory effect of AEA on glucose uptake by increasing the extracellular concentration of AEA and prolonging its binding to CB1 receptors.

Stimulation of glucose uptake by AEA requires NO, but not oxygenation. Previous studies have shown that stimulation of glucose uptake by insulin in skeletal muscle and adipose tissues *in vivo* is NO dependent [50]. In addition, our group has reported that activation of CB1R by AEA in human endothelial cells leads to increased iNOS activity and expression [51]. Therefore, to check the involvement of NO in AEA-stimulated glucose transport, 3T3-L1 adipocytes were incubated with AEA in the presence of the NOS inhibitor L-NAME (20 μM) [51]. This substance was able to reduce the effect of AEA down to ~60% of the controls (Fig. 4b). In contrast, the NO-donor sodium nitroprusside (SNP), used at 50 mM, which releases nanomolar concentrations of NO [52, 53], enhanced glucose transport similar to 10 μM AEA, leading

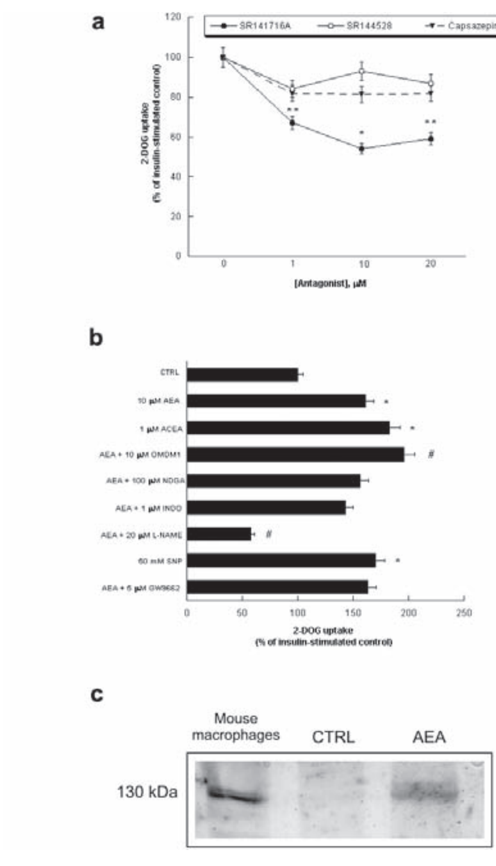

Figure 4. Effect of endocannabinoid-related compounds on AEA-stimulated glucose uptake in 3T3-L1 cells. Adipocytes were incubated for 24 h with (*a*) 10 μM AEA, alone or in the presence of 1 μM SR141716A, 1 μM SR144528 or 10 μM capsazepine, or (*b*) with endocannabinoid-related compounds. (*c*) Western blot analysis of inducible nitric oxide synthase (iNOS) expression in 3T3-L1 adipocytes, incubated for 24 h in the presence or absence of 10 μM AEA. Cell lysates from mouse macrophages stimulated with IFN-γ and LPS were used as positive control. Expected molecular mass of iNOS is reported on the left-hand side. In (*a*, *b*), values were expressed as percentage of glucose uptake in insulin-stimulated controls (100% =302 ± 36 pmol/min per mg protein). Vertical bars represent SD values. In (*a*), * $p < 0.01$ and ** $p < 0.05$ *versus* control. In (*b*), [*] $p < 0.01$ *versus* control, and [#] $p < 0.01$ *versus* 10 μM AEA ($p > 0.05$ in all other cases).

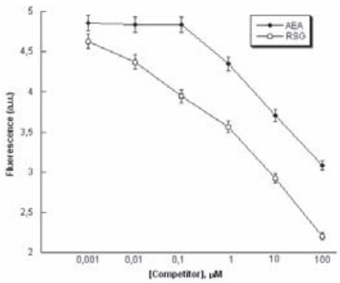

Figure 5. Binding of AEA to PPARγ. Displacement of the fluorescent Fuormone™ PPAR green ligand from the binding pocket of PPARγ by AEA or rosiglitazone (RSG). Fluorescence intensity was expressed in arbitrary units (a.u.). Vertical bars represent SD values.

to a ~170% increase over the controls (Fig. 4b). Taken together, these data demonstrate that NO participates in AEA-stimulated glucose uptake.

Next 3T3-L1 adipocytes on d9 were treated with 10 µM AEA for 24 h to investigate the effect of this endocannabinoid on the expression of iNOS. Since iNOS has been shown to increase in mouse macrophages stimulated with IFN-γ and LPS [42], the latter cells were used as a positive control. Western blot analysis with monoclonal anti-iNOS antibodies recognized a single immunoreactive band of the expected molecular size for iNOS in adipocytes treated with 10 µM AEA, but not in untreated controls (Fig. 4c).

Finally, we checked whether COX-2 and/or LOX could have a role in AEA-stimulated glucose uptake since AEA can be metabolized by COX-2 [33] and LOX [34], generating active products [33, 34]. Fatty acid derivatives generated by these oxygenases are known to interfere with adipocyte metabolism [29–32]. Therefore, the activity of AEA was tested in the presence of 100 µM nordihydroguaiaretic acid (NDGA), a pan-LOX inhibitor [54], or of 1 µM indomethacin (INDO), a pan-COX inhibitor [55]. As shown in Figure 4b, neither NDGA nor INDO affected the activity of AEA, ruling out that oxygenated products of this endocannabinoid were contributing to the modulation of glucose transport.

AEA binding to PPARγ does not affect glucose uptake. To further explore the mechanism underlying the effect of AEA on glucose uptake, we examined a possible role of PPARγ. PPARγ is a key transcriptional factor that controls adipogenesis and glucose homeostasis [35, 56], and recently its activation by AEA has been shown to induce 3T3-L1 fibroblast differentiation into adipocytes [26]. Here, differentiated 3T3-L1 cells were treated for 30 min with 5 µM GW9662, a PPARγ antagonist [57, 58], before the addition of 10 µM AEA. Pre-treatment with GW9662 did not prevent the stimulatory effect of AEA on glucose uptake (Fig. 4b), suggesting that the activity of AEA was independent of PPARγ. Nevertheless, we found by means of displacement assays [26] that AEA was indeed able to bind to PPARγ, in a concentration-dependent manner (Fig. 5). It was also possible to calculate an IC_{50} for AEA, which was 10 µM, in keeping with a recent report [26].

Discussion

In the past few years, evidence has accumulated that points to a role for endocannabinoids in regulating food intake and energy homeostasis [12, 13]. However, the molecular mechanisms underlying the effects of endocannabinoids in adipocyte biology remain largely unclear [11, 14, 18–20]. Here, we investigated whether the endocannabinoid system changes upon adipocyte differentiation, and its possible effect on glucose transport.

The presence and expression of CB1 and CB2 receptors in preadipocytes and differentiated adipocytes was demonstrated by: (i) saturation curves of [^{3}H]CP55.940; (ii) displacement of [^{3}H]CP55.940 binding by selective CB1 or CB2 antagonists; and (iii) cross-reactivity with specific anti-CB1R and anti-CB2R antibodies. Interestingly, the same receptor subtypes have been shown in subcutaneous and omental adipocytes of individuals undergoing liposuction [24], suggesting that they may have a functional role also in humans. In line with this, the fivefold higher expression of CB1R *versus* CB2R in differentiated murine adipocytes (1.700 ± 0.130 *versus* 0.340 ± 0.040 A_{405} units per µg protein) seems to give biochemical support to the therapeutic efficacy of the CB1R antagonist rimonabant for the treatment of obesity [21, 22]. Furthermore, the unprecedented characterization of TRPV1 receptor in 3T3-L1 cells corroborates a preliminary report on the presence of this receptor in human adipose tissue [25], and seems to anticipate a role for TRPV1 in adipocyte biology.

We have also shown that 3T3-L1 preadipocytes and adipocytes are able to degrade AEA through an AMT-dependent uptake, followed by intracellular hydrolysis by FAAH. The presence of these two components of the endocannabinoid system were demonstrated by: (i) kinetic curves of AEA transport or hydrolysis; (ii) inhibition by selective AMT or FAAH inhibitors; (iii) cross-reactivity with specific polyclonal antibodies (for FAAH only). In this context, it should be noted that the molecular properties of a purported AEA membrane transporter are not yet known, and no probes are available to measure the expression of this so-far-putative entity [5, 7, 35]. In addition, we have shown that 3T3-L1 cells have the ability to synthesize AEA via NAPE-PLD activity, an observation that corroborates a recent report on the presence of AEA in these cells [27]. To the best of our knowledge, these data represent the first characterization of a complete and functional AEA-related endocannabinoid system in adipocytes, lending support to the presence of the genes encoding for CB1R, CB2R, NAPE-PLD, and FAAH in these cells [27]. Taken together, our findings may form the basis for a better understanding of the effects of (endo)cannabinoids and related compounds on adipocyte biology [13, 14, 19, 20]. In this context, it seems of utmost importance to further investigate the presence and possible modulation in differentiating adipocytes of the enzymes that synthesize [59] and degrade [60] the other major endocannabinoid 2-AG. This study is currently ongoing in our laboratory and will be the subject of an independent report.

A major finding of this investigation is the observation that differentiation of preadipocytes into adipocytes is paralleled by an increased efficiency of CBR binding. Since the expression of CB1R is almost doubled in differentiated adipocytes, whereas that of CB2R is approximately reduced by half, it can be concluded that the CB1 receptor subtype is the main responsible for the increased binding efficiency. On the other hand, differentiation leads to enhanced AEA degradation by AMT and FAAH, an observation that is in keeping with a role for this endocannabinoid as differentiation-promoting signal [26]. In fact, it can be expected that such a signal has to be disposed at the end of the differentiation process. In this context, it should be stressed that the control of adipocyte differentiation by AEA occurs through PPARγ [26], whereas CB1 receptors are engaged in the control by AEA of insulin-stimulated glucose uptake (this study). Therefore, it is possible that up-regulation of CB1R upon differentiation might be a compensatory mechanism, by which adipocytes keep a suitable CB1R-dependent stimulation of glucose uptake even in the presence of reduced AEA levels. On a general note, the fact that enhanced degradation, rather than reduced synthesis, is the means to control the endogenous tone of AEA extends to 3T3-L1 cells is similar to previous observations on *faah* knockout mice and a number of different cell systems (reviewed in [3, 9]).

Another major finding of this study is the observation that AEA regulates insulin-stimulated glucose uptake in differentiated adipocytes. In line with this, a role for fatty acids in the control of glucose homeostasis and of its dysregulation in diabetes has been known for a long time [22, 61, 62]. Our studies showed that exposure to AEA for 24 h potentiates insulin-stimulated, but not basal, glucose uptake. The potentiation of glucose uptake by AEA was independent of AEA oxygenation by COX or LOX, and also of PPARγ activation. On the contrary, it engaged CB1 receptors, as demonstrated by the ability of the CB1R antagonist SR141716A to minimize the activity of AEA, and by the ability of the CB1R agonist ACEA to mimic it. It seems noteworthy that in a previous report iNOS was shown to be part of the signaling pathway triggered by CB1R in primary endothelial cells [51], and that NO is known to have a crucial role in the regulation of lipolysis [63, 64]. In keeping with this background, we found that the NO-donor SNP mimicked AEA-stimulated glucose uptake, which, in contrast, was reduced by the NOS inhibitor L-NAME. In addition, AEA enhanced iNOS expression in 3T3-L1 adipocytes, overall suggesting that this endocannabinoid plays a role in the regulation of glucose transport by NO [63–65].

In summary, in this investigation we have reported unprecedented evidence that: (i) murine 3T3-L1 preadipocytes and differentiated adipocytes have a functional endocannabinoid system; (ii) some elements of this system (namely CB receptors, AMT and FAAH) are modulated by the differentiation of preadipocytes into adipocytes; and (iii) AEA increases insulin-stimulated glucose uptake by a CB1R- and NO-dependent mechanism. It is noteworthy that our findings strongly support a role for the endocannabinoid system in energy metabolism and fuel storage, and suggest that therapeutics targeted against CB1R or PPARγ might help to dissect the AEA-dependent regulation of glucose uptake from that of adipocyte differentiation, respectively. Such action of AEA on different receptors may also be of therapeutic utility for the treatment of metabolic diseases like hyperglycemia, hyperlipidemia, and type-2 diabetes.

Acknowledgements. The authors wish to thank Prof. Massimo Federici and Dr. Rossella Menghini (University of Rome 'Tor Vergata') for their advice in the preliminary stage of this study. Financial support from Fondazione della Cassa di Risparmio di Teramo (TERCAS 2004), Ministero della Salute (R. C. 2005), Istituto Superiore di Sanità (AIDS Project 2005), and Agenzia Spaziale Italiana (DCMC and MoMa projects 2006) is also gratefully acknowledged.

1 Howlett, A. C., Breivogel, C. S., Childers, S. R., Deadwyler, S. A., Hampson, R. E. and Porrino, L. J. (2004) Cannabinoid physiology and pharmacology: 30 years of progress. Neuropharmacology 47, 345–358.
2 Hermann, H., De Petrocellis, L., Bisogno, T., Schiano Moriello, A., Lutz, B. and Di Marzo, V. (2003) Dual effect of cannabinoid CB1 receptor stimulation on a vanilloid VR1 receptor-mediated response. Cell. Mol. Life Sci. 60, 607–616.
3 Bari, M., Battista, N., Fezza, F., Gasperi, V. and Maccarrone, M. (2006) New insights into endocannabinoid degradation and its therapeutic potential. Mini Rev. Med. Chem. 6, 257–268.
4 Okamoto, Y., Morishita, J., Tsuboi, K., Tonai, T. and Ueda, N. (2004) Molecular characterization of a phospholipase D generating anandamide and its congeners. J. Biol. Chem. 279, 5298–5305.
5 Van der Stelt, M. and Di Marzo, V. (2004) Endovanilloids. Putative endogenous ligands of transient receptor potential vanilloid 1 channels. Eur. J. Biochem. 271, 1827–1834.
6 Hillard, C. J. and Jarrahian, A. (2003) Cellular accumulation of anandamide: consensus and controversy. Br. J. Pharmacol. 140, 802–808.
7 Oddi, S., Bari, M., Battista, N., Barsacchi, D., Cozzani, I. and Maccarrone, M. (2005) Confocal microscopy and biochemical analysis reveal spatial and functional separation between anandamide uptake and hydrolysis in human keratinocytes. Cell. Mol. Life Sci. 62, 386–395.
8 Glaser, S. T., Kaczocha, M. and Deutsch, D. G. (2005) Anandamide transport: a critical review. Life Sci. 77, 1584–604.
9 McKinney, M. K. and Cravatt, B. F. (2005) Structure and function of fatty acid amide hydrolase. Annu. Rev. Biochem. 74, 411–432.

10 Berry, E. M. and Mechoulam, R. (2002) Tetrahydrocannabinol and endocannabinoids in feeding and appetite. Pharmacol. Ther. 95, 185–190.
11 Horvath, T. L. (2003) Endocannabinoids and the regulation of body fat: the smoke is clearing. J. Clin. Invest. 112, 323–336.
12 Di Marzo, V. and Matias, I. (2005) Endocannabinoid control of food intake and energy balance. Nat. Neurosci. 8, 585–589.
13 Pagotto, U., Marsicano, G., Cota, D., Lutz, B. and Pasquali, R. (2006) The emerging role of the endocannabinoid system in endocrine regulation and energy balance. Endocr. Rev. 27, 73–100.
14 Cota, D., Marsicano, G., Lutz, B., Vicennati, V., Stalla, G. K., Pasquali, R. and Pagotto, U. (2003) Endogenous cannabinoid system as a modulator of food intake. Int. J. Obes. Relat. Metab. Disord. 27, 289 –301.
15 Jamshidi, N. and Taylor, D. A. (2001) Anandamide administration into the ventromedial hypothalamus stimulates appetite in rats. Br. J. Pharmacol. 134, 1151–1154.
16 Williams, C. M. and Kirkham, T. C. (1999) Anandamide induces overeating: mediation by central cannabinoid receptors. Psychopharmacology 143, 315–317.
17 Williams, C. M. and Kirkham, T. C. (2002) Observational analysis of feeding induced by Delta9-THC and anandamide. Physiol. Behav. 76, 241–250.
18 Osei-Hyiaman, D., DePetrillo, M., Pacher, P., Liu, J., Radaeva, S., Batkai, S. Harvey-White, J., Mackie, K., Offertaler, L., Wang, L. and Kunos, G. (2005) Endocannabinoid activation at hepatic CB1 receptors stimulates fatty acid synthesis and contributes to diet-induced obesity. J. Clin. Invest. 115, 1298–12305.
19 Bensaid, M., Gary-Bobo, M., Esclangon, A., Maffrand, J. P., Le Fur G, Oury-Donat, F. and Soubrie, P. (2003) The cannabinoid CB1 receptor antagonist SR141716 increases Acrp30 mRNA expression in adipose tissue of obese *fa/fa* rats and in cultured adipocyte cells. Mol. Pharmacol. 63, 908–914.
20 Poirier, B., Bidouard, J. P., Cadrouvele, C., Marniquet, X., Staels, B., O'Connor, S. E. and Herbert, J. M. (2005) The antiobesity effect of rimonabant is associated with an improved serum lipid profile. Diabetes Obes. Metab. 7, 65–72.
21 Vastag, B. (2003) Experimental drugs take aim at obesity. JAMA 289, 1763–1764.
22 Van Gaal, L. F., Rissanen, A. M., Scheen, A. J., Ziegler, O., Rossner, S. (2005) Effects of the cannabinoid-1 receptor blocker rimonabant on weight reduction and cardiovascular risk factors in overweight patients: 1-year experience from the RIO-Europe study. Lancet 365, 1389–1397.
23 Engeli, S., Bohnke, J., Feldpausch, M., Gorzelniak, K., Janke, J., Bàtkai, S. Pacher, P., Harvey-White, J., Luft, F. C., Sharma, A. M. and Jordan, J. (2005) Activation of the peripheral endocannabinoid system in human obesity. Diabetes 54, 2838–2843.
24 Roche, R., Hoareau, L., Bes-Houtmann, S., Gonthier, M. P., Laborde, C., Baron, J. F., Haffaf, Y., Cesari, M. and Festy, F. (2006) Presence of the cannabinoid receptors, CB1 and CB2, in human omental and subcutaneous adipocytes. Histochem. Cell Biol. 4, 1–11.
25 Spoto, B., Fezza, F., Parlongo, G., Battista, N., Sgrò E., Gasperi, V., Zoccali, C. and Maccarrone, M. (2006) Human adipose tissue binds and metabolizes the endocannabinoids anandamide and 2-arachidonoylglycerol. Biochimie (e-published ahead of print on August 22).
26 Bouaboula, M., Hilairet, S., Marchand, J., Fajas, L., Le Fur, G. and Casellas, P. (2005) Anandamide induced PPARgamma transcriptional activation and 3T3-L1 preadipocyte differentiation. Eur. J. Pharmacol. 517, 174–181.
27 Matias, I., Gonthier, M. P., Orlando, P., Martiadis, V., De Petrocellis, L., Cervino, C., Petrosino, S., Hoareau, L., Festy, F., Pasquali, R., Roche, R., Maj, M., Pagotto, U., Monteleone, P. and Di Marzo, V. (2006) Regulation, function and dysregulation of endocannabinoids in models of adipose and beta-pancreatic cells and in obesity and hyperglycemia. J. Clin. Endocrinol. Metab. 91, 3171–3180.
28 Nugent, C., Prins, J. B., Whitehead, J. P., Wentworth, J. M., Chatterjee, V. K. and O'Rahilly, S. (2001) Arachidonic acid stimulates glucose uptake in 3T3-L1 adipocytes by increasing GLUT1 and GLUT4 levels at the plasma membrane. Evidence for involvement of lipoxygenase metabolites and peroxisome proliferator-activated receptor gamma. J. Biol. Chem. 276, 9149–9157.
29 Chatzipanteli, K., Rudolph, S. and Axelrod, L. (1992) Coordinate control of lipolysis by prostaglandin E2 and prostacyclin in rat adipose tissue. Diabetes 41, 927–935.
30 Girouard, H. and Savard, R. (1998) The lack of bimodality in the effects of endogenous and exogenous prostaglandins on fat cell lipolysis in rats. Prostaglandins Other Lipid Mediat. 56, 43–52.
31 Gowri, M. S., Reaven, G. M. and Azhar, S. (1999) Effect of masoprocol on glucose transport and lipolysis by isolated rat adipocytes. Metabolism 48, 411–414.
32 Mater, M. K., Thelen, A. P. and Jump, D. B. (1999) Arachidonic acid and PGE2 regulation of hepatic lipogenic gene expression. J. Lipid Res. 40, 1045–1052.
33 Kozak, K. R., Prusakiewicz, J. J. and Marnett, L. J. (2004) Oxidative metabolism of endocannabinoids by COX-2. Curr. Pharm. Des. 10, 659–667.
34 Van der Stelt, M., Van Kuik, J. A., Bari, M., van Zadelhoff, G., Leeflang, B. R., Veldink, G. A, Finazzi-Agro, A., Vliegenthart, J. F. and Maccarrone, M. (2002) Oxygenated metabolites of anandamide and 2-arachidonoyl-glycerol: conformational analysis and interaction with cannabinoid receptors, membrane transporter and fatty acid amide hydrolase. J. Med. Chem. 45, 3709–3720.
35 Lee, C. H. and Evans, R. M. (2002) Peroxisome proliferator-activated receptor-gamma in macrophage lipid homeostasis. Trends Endocrinol. Metab. 13, 331–335.
36 Maccarrone, M., Barboni, B., Paradisi, A., Bernabo, N., Gasperi, V. and Pistilli, M. G. (2005) Characterization of the endocannabinoid system in boar spermatozoa and implications for sperm capacitation and acrosome reaction. J. Cell. Sci. 118, 4393–4404.
37 Ross, R. A., Gibson, T. M., Brockie, H. C., Lesile, M., Pashmi, G., Craib, S. J. Di Marzo, V. and Pertwee, R. G. (2001) Structure-activity relationship for the endogenous cannabinoid, anandamide, and certain of its analogues at vanilloid receptors in transfected cells and vas deferens. Br. J. Pharmacol. 132, 631–640.
38 Maccarrone, M., Di Rienzo, M., Battista, N., Gasperi, V., Guerrieri, P. and Rossi, A. (2003) The endocannabinoid system in human keratinocytes. Evidence that anandamide inhibits epidermal differentiation through CB1 receptor-dependent inhibition of protein kinase C, activation protein-1, and transglutaminase. J. Biol. Chem. 278, 33896–33903.
39 Pertwee, R. G. (1997) Pharmacology of cannabinoid CB1 and CB2 receptors. Pharmacol. Ther. 74, 129–180.
40 Fezza, F., Gasperi, V., Mazzei, C. and Maccarrone, M. (2005) Radiochromatographic assay of *N*-acyl-phosphatidylethanolamine-specific phospholipase D (NAPE-PLD) activity. Anal. Biochem. 339, 113–120.
41 Yang, J., Clark, A. E., Kozka, I. J., Cushman, S. W. and Holman, G. D. (1992) Development of an intracellular pool of glucose transporters in 3T3-L1 cells. J. Biol. Chem. 267, 10393–10399.
42 Xie, Q. W., Cho, H. J., Calaycay, J., Mumford, R. A., Swiderek, K. M., Lee, T. D., Ding, A., Troso, T. and Nathan, C. (1992) Cloning and characterization of inducible nitric oxide synthase from mouse macrophages. Science 256, 225–228.
43 Maccarrone, M., Lorenzon, T., Bari, M., Melino, G. and Finazzi-Agrò A. (2000) Anandamide induces apoptosis in human

cells via vanilloid receptors. Evidence for a protective role of cannabinoid receptors. J. Biol. Chem. 275, 31938–31945.
44 Battista, N., Gasperi, V., Fezza, F. and Maccarrone, M. (2005) The anandamide membrane transporter and the therapeutic implications of its inhibition. Therapy 2, 141–150.
45 Ortar, G., Ligresti, A., De Petrocellis, L., Morera, E. and Di Marzo, V. (2003) Novel selective and metabolically stable inhibitors of anandamide cellular uptake. Biochem. Pharmacol. 65, 1473–1481.
46 De Petrocellis, L., Bisogno, T., Maccarrone, M., Davis, J. B., Finazzi-Agrò, A. and Di Marzo, V. (2001) The activity of anandamide at vanilloid VR1 receptors requires facilitated transport across the cell membrane and is limited by intracellular metabolism. J. Biol. Chem. 276, 12856–12863.
47 Sipe, J. C., Waalen, J., Gerber, A. and Beutler, E. (2005) Overweight and obesity associated with a missense polymorphism in fatty acid amide hydrolase (FAAH). Int. J. Obes. 29, 755–759.
48 Abadji, V., Lin, S., Taha, G., Griffin, G., Stevenson, L. A., Pertwee, R. G. and Makriyannis, A. (1994) (R)-methanandamide: a chiral novel anandamide possessing higher potency and metabolic stability. J. Med. Chem. 37, 1889–1893.
49 Hillard, C. J., Manna, S., Greenberg, M. J., DiCamelli, R., Ross, R. A., Stevenson, L. A. Murphy, V., Pertwee, R. G. and Campbell, W. B. (1999) Synthesis and characterization of potent and selective agonists of the neuronal cannabinoid receptor (CB1). J. Pharmacol. Exp. Ther. 289, 1427–1433.
50 Roy, D., Perreault, M. and Marette, A. (1998) Insulin stimulation of glucose uptake in skeletal muscles and adipose tissues in vivo is NO dependent. Am. J. Physiol. 274, 692–699.
51 Maccarrone, M., Bari, M., Lorenzon, T., Bisogno, T., Di Marzo, V. and Finazzi-Agrò A. (2000) Anandamide uptake by human endothelial cells and its regulation by nitric oxide. J. Biol. Chem. 275, 13484–13492.
52 Bauer, J. A., Booth, B. P. and Fung, H. L. (1995) Nitric oxide donors: biochemical pharmacology and therapeutics. Adv. Pharmacol. 34, 361–381.
53 Matthews, J. R. Botting, C. H., Panico, M., Morris, H. R. and Hay, R. T. (1996) Inhibition of NF-kappaB DNA binding by nitric oxide. Nucleic Acids Res. 24, 2236–2242.
54 Tobias, L. D. and Hamilton, J. G. (1979) The effect of 5,8,11,14-eicosatetraynoic acid on lipid metabolism. Lipids 14, 181–193.
55 Shen, T. Y. and Winter, C. A. (1977) Chemical and biological studies on indomethacin, sulindac and their analogs. Adv. Drug. Res. 12, 290–245.
56 Marx, N., Duez, H., Fruchart, J. C. and Staels, B. (2004) Peroxisome proliferator-activated receptors and atherogenesis: regulators of gene expression in vascular cells. Circ. Res. 94, 1168–1178.
57 Leesnitzer, L. M., Parks, D. J., Bledsoe, R. K., Cobb, J. E., Collins, J. L., Consler, T. G. Davis, R. G., Hull-Ryde, E. A., Lenhard, J. M., Patel, L., Plunket, K. D., Shenk, J. L., Stimmel, J. B., Therapontos C, Willson, T. M. and Blanchard, S. G. (2002) Functional consequences of cysteine modification in the ligand binding sites of peroxisome proliferator activated receptors by GW9662. Biochemistry 41, 6640–6650.
58 Seargent, J. M., Yates, E. A. and Gill, J. H. (2004) GW9662, a potent antagonist of PPARgamma, inhibits growth of breast tumour cells and promotes the anticancer effects of the PPARgamma agonist rosiglitazone, independently of PPARgamma activation. Br. J. Pharmacol. 143, 933–937.
59 Bisogno, T., Howell, F., Williams, G., Matias, I., Schiano-Moriello, A., Paul, P., Williams, E. J., Gangadharan, U., Hobbs, C., Di Marzo, V. and Doherty, P. (2003) Cloning of the first sn1-DAG lipases points to the spatial and temporal regulation of endocannabinoid knockout in the brain. J. Cell Biol. 163, 463–468.
60 Dinh, T. P., Carpenter, D., Lesle, F. M., Freund, T. F., Katona, I., Sensi, S. L., Kathuria, S. and Piomelli, D. (2002) Brain monoglyceride lipase participating in endocannabinoid inactivation. Proc. Natl. Acad. Sci. USA 99, 10819–10824.
61 Grunfeld, C., Baird, K. L. and Kahn, C. R. (1981) Maintenance of 3T3-L1 cells in culture media containing saturated fatty acids decreases insulin binding and insulin action. Biochem. Biophys. Res. Commun. 103, 219–226.
62 Fong, J. C., Chen, C. C., Liu, D., Chai, S. P., Tu, M. S. and Chu, K. Y. (1996) Arachidonic acid stimulates the intrinsic activity of ubiquitous glucose transporter (GLUT1) in 3T3-L1 adipocytes by a protein kinase C-independent mechanism. Cell Signal. 8, 179–183.
63 Tanaka, T., Nakatani, K., Morioka, K., Urakawa, H., Maruyama, N., Kitagawa, N., Katsuki, A., Araki-Sasaki, R., Hori, Y., Gabazza, E. C., Yano, Y., Wada, H., Nobori, T., Sumida, Y. and Adachi, Y. (2003) Nitric oxide stimulates glucose transport through insulin-independent GLUT4 translocation in 3T3-L1 adipocytes. Eur. J. Endocrinol. 149, 61–67.
64 Li, J., Hu, X., Selvakumar, P., Russell, R. R., Cushman, S. W., Holman, G. D. and Young, L. H. (2004) Role of the nitric oxide pathway in AMPK-mediated glucose uptake and GLUT4 translocation in heart muscle. Am. J. Physiol. Endocrinol. Metab. 287, 834–841.
65 Engeli, S., Janke, J., Gorzelniak, K., Bohnke, J., Ghose, N., Lindschau, C., Luft, F. C. and Sharma, A. M. (2004) Regulation of the nitric oxide system in human adipose tissue. J. Lipid Res. 45, 1640–1648.